Towards a Comprehensive Model for the Impact of Traffic Patterns on Air Pollution

Caterina Balzotti[1], Maya Briani[2], Barbara de Filippo[2] and Benedetto Piccoli[3]

[1]*SBAI Department, Sapienza Università di Roma, Rome, Italy*
[2]*Consiglio Nazionale delle Ricerche, Istituto per le Applicazioni del Calcolo M. Picone, Rome, Italy*
[3]*Department of Mathematical Sciences, Rutgers University, Camden, U.S.A.*

Keywords: Road Traffic Modeling, Second Order Traffic Model, Air Pollutant Emissions, Ozone Production.

Abstract: The impact of vehicular traffic on society is huge and multifaceted, including economic, social, health and environmental aspects. The problems is complex and hard to model since it requires to consider traffic patterns, air pollutant emissions, and the chemical reactions and dynamics of pollutants in the low atmosphere. This paper aims at exploring a comprehensive simulation tool ranging from vehicular traffic all the way to environmental impact. As first step in this direction, we couple a traffic second-order model, tuned on NGSIM data, with an nitrogen oxides (NO_x) emission model and a set of equations for some of the main chemical reactions behind ozone (O_3) production.

1 INTRODUCTION

The impact of road traffic and its inefficiencies on society is well known and was documented with quantitative estimates for more than a decade. In 2007, in the sole US, traffic phenomena (such as congestion) contributed for an economic loss of $78 billion. The latter was estimated in the form of 4.2 billion lost hours for delays and 2.9 billion gallons of wasted fuel (TRB Executive Committee, 2013). Moreover, the societal impact is high also in terms of pollution and environmental effects, with road traffic accounting for nearly one third of carbon dioxide (CO_2) emissions (TRB Executive Committee, 2011). While CO_2 is probably one of the most studied molecules, the effect on health is also related to other pollutants, such as particulate matters and nitrogen dioxide (NO_2), see (Zhang and Batterman, 2013). In this paper we focus on the production of ozone (O_3) which is strictly connected with the NO_x gases in the atmosphere (Atkinson, 2000; Wang et al., 2017; Chameides et al., 1988).

New technologies have the possibility of contributing to reduce such heavy toll and even small improvements (in relative terms) in this polluted areas will contribute to substantial economic and environmental positive impact. Notice that much attention has been devoted in traffic literature to quantities such as flow, capacity and travel time. However, advanced modeling of fuel consumption and emission still faces limitations, especially for tools which can be integrated with the increasing flow of data from probe sensors. One of the main reasons is the high variability of fuel consumption and emissions, which are influenced by many factors as the vehicle type, make, model, year and others.

Interestingly, traffic patterns, such as congestion and traveling waves, account for large variations in fuel consumption, and consequently emissions, but smaller ones for flow and travel times. Therefore, improvement in terms of traffic patterns will mostly affect fuel consumption and emissions, rather than traveling times. For instance, it was shown via simulation that a small number of autonomous and connected vehicles may contribute to reduce the formation of traffic waves and smooth traffic flow, see (Davis, 2004; Talebpour and Mahmassani, 2016; Guériau et al., 2016; Wang et al., 2016; Knorr et al., 2012). Moreover, experimental evidence showed that this results in significant reduction of fuel consumption and emissions, see (Stern et al., 2018; Stern et al., 2019). A key point is that many results show how even at very low penetration (i.e. percentage of vehicles which are autonomous or connected) the effect may be of great significance. Similar benefits may be achieved by improving driving efficiency, however this approach needs the development of robust information flow to the drivers or the use of specialized fleets.

221

Despite this success, a comprehensive and advanced evaluation tool, which simulates benefits from traffic regularization, is still lacking. Current estimates are mainly based on statistical analysis of scarce sample data. However, a sound validation of these results at large scale requires the development of a comprehensive tool, which will model the various aspects of the problem, ranging from traffic flow all the way to evaluation of pollutant effects on the environment. This paper aims at giving a first attempt for the construction of such tool and provides a general approach to connect traffic simulations to chemical reactions.

2 A MODULAR APPROACH TO EVALUATE TRAFFIC IMPACT

We propose a modular approach as shown in Figure 1.

Figure 1: A Schematic Representation of the Modular Approach.

The modules are the following:

- Traffic simulator
- Fuel consumption and emissions model
- Chemical reactions model
- Diffusion and transportation model
- Impact evaluation module (e.g. monument degradation, health impact, other)

The first module aims at simulating the load of a road network on a given time scale, which can range from few hours to weeks. We propose to use macroscopic traffic models, described in detail in Section 3, which can be fed by mobile sensors data (Work et al., 2010). The second module will be based on the use of pollutant emission rate estimators, which can use measurements and data produced by module one for aggregated estimates, see (Piccoli et al., 2015). The third module needs to be developed in dependence of the considered pollutants, while the fourth is based on reaction-diffusion models using partial differential equations (Alvarez-Vázquez et al., 2017; Samaranayake et al., 2014). Finally, last module is highly dependent on the considered impact.

In this paper, we focus on the first three modules, aiming to give a possible approach to evaluate the impact of vehicular traffic on the production of ozone.

3 TRAFFIC MODEL

Depending on the scale at which traffic models represent vehicular traffic, they are divided in the following categories: *cellular*, each road is represented by cells which may contain more vehicles (Nagel and Schreckenberg, 1992; Fukui and Ishibashi, 1996; Daganzo, 2006; Sakai et al., 2006; Alperovich and Sopasakis, 2008); *microscopic*, individual vehicles dynamics are modeled by ordinary differential equations (Pipes, 1953; Newell, 1961; Bando et al., 1995) and *continuum*, where the car density evolves according to a partial differential equation, which can be of kinetic type (Herman and Prigogine, 1971; Phillips, 1979; Klar and Wegener, 2000; Illner et al., 2003) or fluid-dynamic ones (Lighthill and Whitham, 1955; Richards, 1956; Kerner and Konhäuser, 1993; Kerner and Konhäuser, 1994; Aw and Rascle, 2000). For a deeper review see (Helbing, 2001; Albi et al., 2019; Garavello et al., 2016; Piccoli and Tosin, 2011).

The different classes of models have advantages and disadvantages. We focus on macroscopic fluid-dynamic ones. Such models are based on the conservation of vehicles, $\rho_t + (\rho v)_x = 0$, where $\rho(x,t)$ is the vehicle density and $v(x,t)$ the average velocity. The *first order* Lighthill-Whitham-Richards (LWR) model (Lighthill and Whitham, 1955; Richards, 1956) assumes a functional relationship between velocity and density, $v = v(\rho)$, and yields the LWR PDE

$$\rho_t + f(\rho)_x = 0 \, , \qquad (1)$$

where $f = \rho v(\rho)$ is the flow rate of vehicles. *Second order models* consider ρ and v as independent quantities and consist of balance laws

$$\begin{cases} \rho_t + (\rho v)_x = 0 \\ v_t + f(\rho, v)_x = A(\rho, v), \end{cases} \qquad (2)$$

where A is an acceleration term. Among the most used models we recall the Aw-Rascle-Zhang (ARZ) model (Aw and Rascle, 2000; Greenberg, 2001; Zhang, 2002). These models are able to capture the formation of traffic waves from steady traffic situations (known also as *phantom traffic jams*) which are observed experimentally (Sugiyama et al., 2008). Such waves are responsible for breaking events, the increase in fuel consumption and many other drawbacks with environmental effects. For these reasons in this paper we adopt second order models to simulate complex traffic situations which are the main responsible of pollutant emissions.

Specifically, we use the second order *Collapsed Generalized Aw-Rascle-Zhang* (CGARZ) model (Fan et al., 2017; Fan, 2013), to describe the evolution of traffic flow. The CGARZ model belongs to the

family of macroscopic *Generic Second Order Models* (GSOM) (Lebacque et al., 2007), which satisfy

$$\begin{cases} \rho_t + (\rho v)_x = 0 \\ w_t + v w_x = 0, \end{cases} \tag{3}$$
$$\text{with } v = V(\rho, w),$$

for a specific velocity function V. Here $\rho(x,t)$ is the traffic density, $v(x,t)$ the velocity and and $w(x,t)$ is a property of vehicles which is advected by traffic flow. GSOM are characterized by a family of fundamental diagrams $f(\rho, w) = \rho V(\rho, w)$, parametrized by w. The peculiarity of the CGARZ model is that it possesses a single-valued fundamental diagram in free-flow, and a multi-valued function in congestion. Here, we use the flux and velocity functions proposed in (Balzotti et al., 2019).

4 EMISSIONS

In this section we introduce an emission model suitable for several air pollutants. Specifically, we focus on ozone (O_3) and nitrogen oxides (NO_x) which are of particular interest in areas with heavy vehicular traffic and high amounts of UV radiation. Ozone is a secondary pollutant and its production is due to a complex system of reactions of its precursors, mainly NO_x gases, in a sunlight ambient, (Jacob, 2000; Song et al., 2011).

Starting from the model proposed in (Panis et al., 2006), we assume to have N vehicles in a stretch of road going all at the same speed $\bar{v}$, with the same acceleration $\bar{a}$. Then, the emission rate $E(t)$ at time t is given by the N contributes of the vehicles, such that

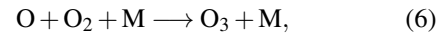$$\begin{aligned} E(t) = N \max\{ & E_0, f_1 + f_2 \bar{v}(t) + f_3 \bar{v}(t)^2 \\ & + f_4 \bar{a}(t) + f_5 \bar{a}(t)^2 + f_6 \bar{v}(t) \bar{a}(t) \}, \end{aligned} \tag{4}$$

where E_0 is a lower-bound of emission and f_1 to f_6 are emission constants. See (Panis et al., 2006, Table 2) for the NO_x estimated coefficients. In this work, the velocity and acceleration quantities in equation (4) are provided by the numerical solution to the CGARZ model (3). We refer to (Balzotti et al., 2019) for the validation of the proposed approach.

5 CHEMICAL REACTIONS

In this section we are interested in the main chemical reactions of nitrogen oxides which lead to the production of ozone. Ozone is produced in the troposphere by a complex reaction mechanism that involves mainly volatile organic compounds and NO_x

(Jacob, 2000). Nitrogen oxides is a collective term used to refer to nitrogen oxide (NO) and nitrogen dioxide (NO_2), that are usually produced from fuel combustion in car engines, especially at high temperatures (Omidvarborna et al., 2015). Classified as a secondary pollutant, NO_2 is a very reactive compound that can be photo-dissociated and produce atomic oxygen (O) that quickly combines with an oxygen molecule to form an ozone molecule. This complex mechanism is considered one of key steps in the formation of ground-level ozone. In polluted regions with high vehicle emissions, NO_2 is a relevant precursor substance for the ozone in photochemical smog and the ozone production is due to the following reactions

$$NO_2 + h\nu \longrightarrow O + NO \tag{5}$$
$$O + O_2 + M \longrightarrow O_3 + M, \tag{6}$$

where h is Planck's constant and ν the frequency. M is a chemical species, such as oxygen (O_2) or nitrogen (N_2), that adsorbs the excess of energy generated in reaction (6), (Manahan, 2017). Moreover, in presence of NO, O_3 reacts with it and this reaction destroys the ozone and reproduces the NO_2,

$$O_3 + NO \longrightarrow O_2 + NO_2. \tag{7}$$

This means that the previous reactions do not result in net ozone production, indeed reactions (6) and (7) balance the cycle between NO_x and O_3. The complexity of the ground-level ozone production, that involves many different precursors such as VOC, NO_x and others, forces us to focus on a simple subset of chemical reactions not taking into account important aspects such as diurnal/nocturnal variation and their relative dispersion, see (Song et al., 2011).

5.1 Estimating the Production of O_3

In this section we define a model consisting in as system of ordinary differential equation to represent the ozone production resulting from traffic emissions. More precisely, we set up ordinary differential equations for each of the chemical reactions introduced in (5), (6) and (7). We denote the chemical species concentration by $[\cdot] = [\text{weight unit}/\text{volume unit}]$.

We assume that the first reaction (5) takes place only during the daily hours with a fixed *kinetic constant* k_1. Thus the associated system of ODE is

$$\begin{aligned} \frac{d[NO_2]}{dt} &= -k_1[NO_2] \\ \frac{d[O]}{dt} &= k_1[NO_2] \\ \frac{d[NO]}{dt} &= k_1[NO_2]. \end{aligned} \tag{8}$$

For the second reaction (6) we choose M to be O_2, then

$$O + 2O_2 \longrightarrow O_3 + O_2$$

and we call k_2 the associated kinetic constant. We obtain the system

$$
\begin{aligned}
\frac{d[O]}{dt} &= -k_2[O]\,[O_2]^2 \\
\frac{d[O_2]}{dt} &= -k_2[O]\,[O_2]^2 \\
\frac{d[O_3]}{dt} &= k_2[O]\,[O_2]^2.
\end{aligned}
\tag{9}
$$

The third reaction (7) gives us the third system of ODEs with kinetic constant k_3

$$
\begin{aligned}
\frac{d[O_3]}{dt} &= -k_3[O_3]\,[NO] \\
\frac{d[NO]}{dt} &= -k_3[O_3]\,[NO] \\
\frac{d[O_2]}{dt} &= k_3[O_3]\,[NO] \\
\frac{d[NO_2]}{dt} &= k_3[O_3]\,[NO].
\end{aligned}
\tag{10}
$$

Finally, we combine the systems (8), (9) and (10) into a unique set of equations, adding the contribution of the traffic emissions. We assume that the reactions take place in a volume of dimension Δx^3, and the traffic emissions contribution acts as a source term for the concentration of NO and NO_2. Hence, we define the variation of the concentration of NO_x in Δx^3, at each time t as

$$S_{NO_x} = \frac{E_{NO_x}(t)}{\Delta x^3}, \tag{11}$$

where the emission rate $E_{NO_x}(t)$ is given by (4). The final system then becomes

$$
\begin{aligned}
\frac{d[O]}{dt} &= -k_2[O]\,[O_2]^2 &+& k_1[NO_2] \\
\frac{d[O_2]}{dt} &= -k_2[O]\,[O_2]^2 &+& k_3[O_3]\,[NO] \\
\frac{d[O_3]}{dt} &= k_2[O]\,[O_2]^2 &-& k_3[O_3]\,[NO] \\
\frac{d[NO]}{dt} &= k_1[NO_2] &-& k_3[O_3]\,[NO] \\
&\; +(1-p)S_{NO_x} \\
\frac{d[NO_2]}{dt} &= -k_1[NO_2] &+& k_3[O_3]\,[NO] \\
&\; +pS_{NO_x},
\end{aligned}
\tag{12}
$$

where p is the percentage of NO_2 derived from the emission rate of NO_x.

6 NUMERICAL TESTS

In this section we give some tests to illustrate how the first three modules in Figure 1 are combined to estimate the production of ozone.

Let us start by considering the CGARZ traffic model (3) on a road parametrized by the interval $[0,L]$ on a time horizon $[0,T]$. We assume a constant left boundary condition $\rho(0,t) = u_0$, $\forall\, t \in [0,T]$, and we allow all vehicles to leave the road on the right. The parameters used in all simulations are $T = 30\,\mathrm{min}$, $L = 10\,\mathrm{km}$, maximum vehicles velocity allowed $V^{\max} = 120\,\mathrm{km/h}$, road capacity $\rho^{\max} = 133\,\mathrm{veh/km}$, $u_0 = 42\,\mathrm{veh/km}$ and the initial density ρ_0 is

$$\rho_0(x) = \begin{cases} 42 & 0 \le x \le \ell \\ 110 & \ell < x \le L \end{cases} \tag{13}$$

with $\ell = 4.5\,\mathrm{km}$.

6.1 From Traffic Quantities to NO_x Emissions

We divide our domain into cells, with space step Δx and time step Δt. For each cell centered at x_j and time t^n of the numerical grid, we compute the vehicles density ρ_j^n and speed V_j^n using the Godunov-type second order cell transmission scheme (Fan et al., 2017) to solve the CGARZ system (3).

To estimate the NO_x emission rate (4), we need to compute the acceleration of vehicles. Following the approach proposed in (Luspay et al., 2010; Zegeye et al., 2013), which distinguishes between the *temporal acceleration* and the *spatial-temporal acceleration*, we apply the resulting acceleration formula

$$A_i^k = \frac{V_i^{k+1} - V_i^k}{\Delta t} + V_i^k \frac{V_{i+1}^{k+1} - V_i^{k+1}}{\Delta x}. \tag{14}$$

We set now $\Delta x = 0.1\,\mathrm{km}$ and $\Delta t = 0.5\Delta x/V^{\max}$ and starting by initial data (13) we have a traffic dynamic described by a shock wave which propagates backward from the middle of the road, until the interaction with the rarefaction wave stemming from the right, changes the shock speed to positive. The corresponding variation in time of the total emission of NO_x, defined as the sum on the cells of the NO_x emission rates, increases until the traffic dynamic is represented by the shock wave and then it starts to decrease to its lower-bound defined by null acceleration.

We are now interested in studying the effects of traffic lights on the previous dynamic. Specifically, we test the impact on NO_x emissions of different traffic light cycles varying the time frame of the red phase, which corresponds to a condition that imposes

vanishing outflow on the right boundary of the domain. Let t_g and t_r be the time of the green and red traffic light phase respectively. To show the influences of traffic lights on NO_x emissions, we vary t_g and t_r fixing their ratio to $3/2$. In Figure 2 we show the NO_x emissions during 15 minutes of traffic light on. In particular, on the top we set $t_g = 4.5$ min and $t_r = 3$ min, in the center $t_g = 3$ min and $t_r = 2$ min and on the bottom $t_g = 1.5$ min and $t_r = 1$ min. We observe that the duration of the traffic light $t_g + t_r$ has an high influence on the maximum value of the total NO_x emission rate, indeed it grows with the increase of the vehicles restarts.

6.2 Production of Ozone

In this section we use system (12) to estimate the concentration of ozone along the entire road. Following (Jacobson, 2005), we fix the reaction rate parameters as $k_1 = 0.02 \, \text{s}^{-1}$, $k_2 = 6.09 \times 10^{-34} \, \text{cm}^6/\text{molecule}$ and $k_3 = 1.81 \times 10^{-14} \, \text{cm}^3/\text{molecule}$.

For each cell x_j, we set the initial concentrations as:

$$[O] = [O_3] = 0,$$

$$[O_2] = 5.02 \times 10^{18} \, \text{molecule}/\text{cm}^3,$$

and, for NO and NO_2 we use the relation (11) such that at the initial time $t = 0$

$$[NO] = (1 - p) \frac{E_{NO_x}(0)}{\Delta x^3},$$

$$[NO_2] = p \frac{E_{NO_x}(0)}{\Delta x^3},$$

with $p = 0.15$ according to (Carslaw et al., 2011).

For each time step n, we then compute the source term (11) due to traffic by using the NO_x emission rate obtained in the previous tests cases with and without traffic lights, and we solve the ODEs system (12) in each cell x_j.

In Figure 3, we show the O_3 evolution along the entire road, during 15 minutes of simulation. As to be expected, we observe a different behavior in presence or not of the traffic lights and a higher O_3 concentration with traffic light on.

In Figure 4 we compare the variation in time of the total concentration of O_3 in the case of dynamic without traffic lights with the case with traffic light on defined by $t_g = 3$ min and $t_r = 2$ min. As expected, the ozone concentration is amplified by the presence of the traffic lights.

6.3 Weekly Ozone Production

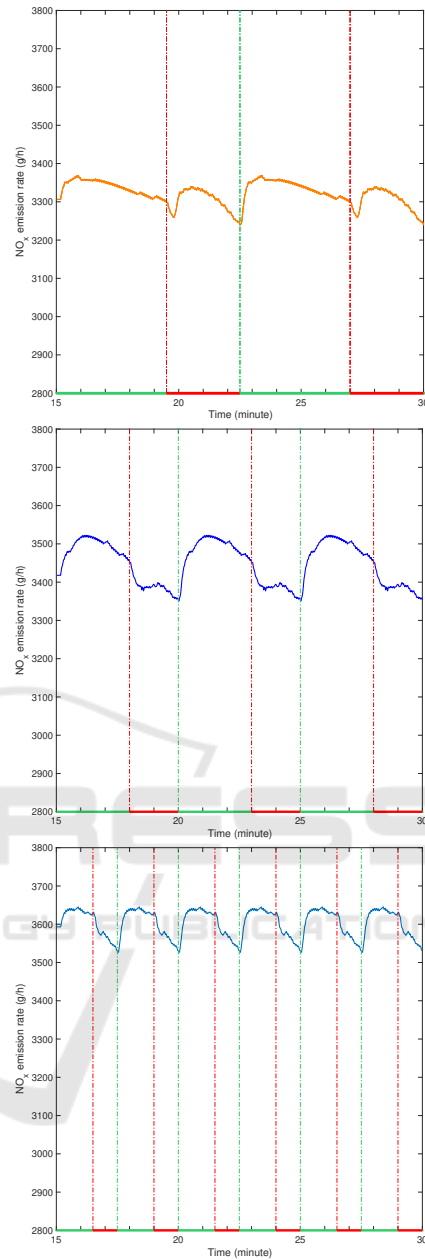In this section we estimate the production of ozone and of the other chemical species during a whole

Figure 2: Variation in Time of the Total NO_x Emission Rate along the Entire Road with $t_g/t_r = 3/2$ and Varying the Traffic Light Duration: (Top) $t_g = 4.5$ min and $t_r = 3$ min; (Center) $t_g = 3$ min and $t_r = 2$ min; (Bottom) $t_g = 1.5$ min and $t_r = 1$ min.

week. Day and night are simulated by varying the kinetic constant k_1 associated to reaction (5) which represents the photo-dissociation of NO_2 by sunlight. The results of our model are to be taken with care because, as noticed above, we did not include all complex chemical reactions happening in the atmosphere. In particular we can not use such results to compare
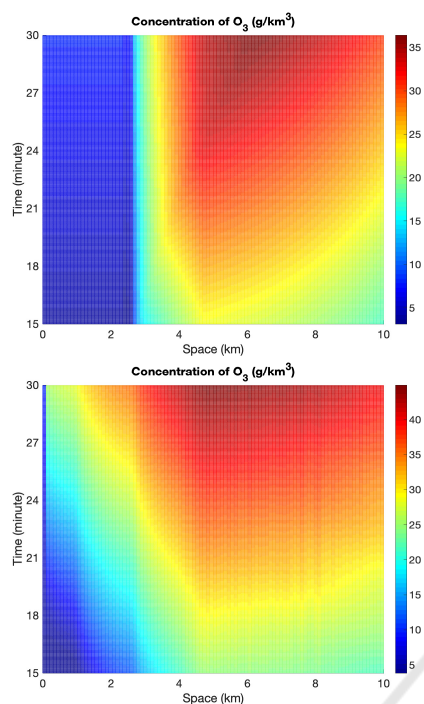
Figure 3: O_3 Evolution along the Entire Road, for 15min of Simulation, in the Case of Dynamics without (Top) and with (Bottom) Traffic Light.
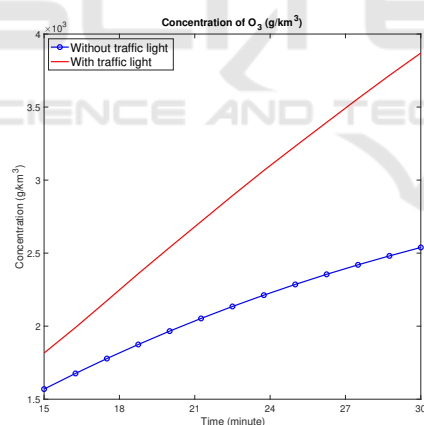

Figure 4: Variation in Time of the Total Concentration of O_3 in the Case of Dynamics with (Red-Solid) and without (Blue-Circles) Traffic Light.

with data from air pollution sensors. However, our scope is to compare production of NO_x and O_3 as due to different traffic patterns. So our analysis is intended a first step in understanding the impact on pollution of traffic lights. In Figure 5 we show the hypothetical trend of parameter k_1 as a Gaussian function of time. We then solve system (12) assuming that the source term S_{NO_x} due to traffic has a similar trend of k_1 during day and night, see again Figure 5. Specifically, the maximum of S_{NO_x} is computed by the mean of the

values during its periodical trend when traffic lights on (see Figure 2).

To further investigate the impact of the traffic light on emissions, we compute the weekly total amount of the considered chemical species. In Figures 6 and 7 we compare the concentration in presence of the traffic light (red-solid line) with respect to the one obtained in the case without traffic light (blue-circles line) for NO and NO_2 respectively. We observe that NO and NO_2 productions are highly amplified by the presence of the traffic light. The dynamic of O_3 is different, since it reaches its saturation value each day at 3 p.m. (in accordance to the time in which the parameter k_1 in Figure 5 is maximum) regardless the presence or not of the traffic light.
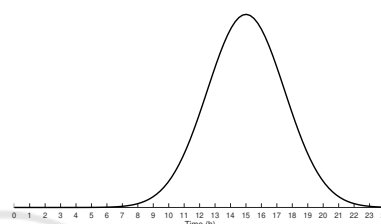

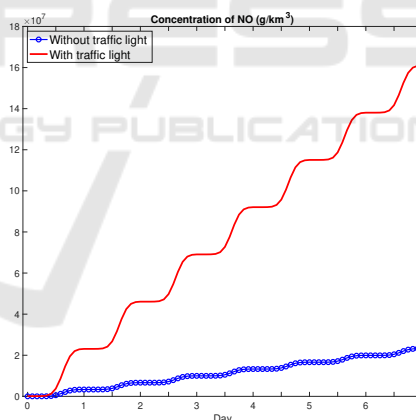Figure 5: Daily Hypothetical Trend of Parameter k_1 and of the Source Term S_{NO_x} as a Function of Time.

Figure 6: Total Production of NO Due to Traffic during a Whole Week with (Red-Solid) and without (Blue-Circles) Traffic Light.

7 CONCLUSIONS

The impact of air quality on public health is one of the world's worst open problems. Emissions from vehicles is one of the major source of the detected air pollutants. In this paper we coupled a CGARZ second-order traffic model with an estimator for NO_x emission rate and a system of equations representing some of the main chemical reactions responsible for
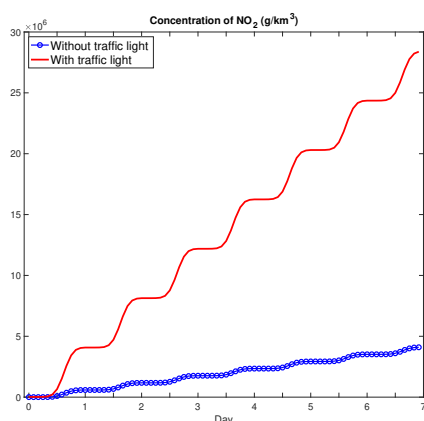
Figure 7: Total Production of NO_2 Due to Traffic during a Whole Week with (Red-Solid) and without (Blue-Circles) Traffic Light.

the ozone production. Future investigations will include pollutant diffusion and transportation in the air and other chemical reactions. Moreover, we aim at extending the tool to road network to better capture environmental effects.

REFERENCES

Albi, G., Bellomo, N., Fermo, L., Ha, S.-Y., Kim, J., Pareschi, L., Poyato, D., and Soler, J. (2019). Vehicular traffic, crowds, and swarms: from kinetic theory and multiscale methods to applications and research perspectives. *Math. Models Methods Appl. Sci.*, 29(10):1901–2005.

Alperovich, T. and Sopasakis, A. (2008). Modeling highway traffic with stochastic dynamics. *J. Stat. Phys*, 133:1083–1105.

Alvarez-Vázquez, L. J., García-Chan, N., Martínez, A., and Vázquez-Méndez, M. E. (2017). Numerical simulation of air pollution due to traffic flow in urban networks. *J. Comput. Appl. Math.*, 326:44–61.

Atkinson, R. (2000). Atmospheric chemistry of VOCs and NO_x. *Atmos. Environ.*, 34(12–14):2063–2101.

Aw, A. and Rascle, M. (2000). Resurrection of "Second Order" Models of Traffic Flow. *SIAM J. Appl. Math.*, 60:916–944.

Balzotti, C., Briani, M., De Filippo, B., and Piccoli, B. (2019). Evaluation of NO_x emissions and ozone production due to vehicular traffic via second-order models. *arXiv preprint arXiv:1912.05956*.

Bando, M., Hesebem, K., Nakayama, A., Shibata, A., and Sugiyama, Y. (1995). Dynamical model of traffic congestion and numerical simulation. *Phys. Rev. E*, 51(2):1035–1042.

Carslaw, D. C., Beevers, S. D., Tate, J. E., Westmoreland, E. J., and Williams, M. L. (2011). Recent evidence concerning higher NO_x emissions from passenger cars and light duty vehicles. *Atmos. Environ.*, 45(39):7053–7063.

Chameides, W. L., Lindsay, R. W., Richardson, J., and Kiang, C. S. (1988). The role of biogenic hydrocarbons in urban photochemical smog: Atlanta as a case study. *Science*, 241(4872):1473–1475.

Daganzo, C. F. (2006). In traffic flow, cellular automata = kinematic waves. *Transp. Res. B*, 40:396–403.

Davis, L. (2004). Effect of adaptive cruise control systems on traffic flow. *Physical Review E*, 69(6):066110.

Fan, S. (2013). *Data-Fitted Generic Second Order Macroscopic Traffic Flow Models*. Ph.D. Thesis, Temple University.

Fan, S., Sun, Y., Piccoli, B., Seibold, B., and Work, D. B. (2017). A Collapsed Generalized Aw-Rascle-Zhang Model and its Model Accuracy. *arXiv preprint arXiv:1702.03624*.

Fukui, M. and Ishibashi, Y. (1996). Traffic Flow in 1D Cellular Automaton Model Including Cars Moving with High Speed. *J. Phys. Soc. Japan*, 65(6):1868–1870.

Garavello, M., Han, K., and Piccoli, B. (2016). *Models for Vehicular Traffic on Networks*. American Institute of Mathematical Sciences.

Greenberg, J. M. (2001). Extension and amplification of the Aw-Rascle model. *SIAM J. Appl. Math.*, 63:729–744.

Guériau, M., Billot, R., El Faouzi, N.-E., Monteil, J., Armetta, F., and Hassas, S. (2016). How to assess the benefits of connected vehicles? A simulation framework for the design of cooperative traffic management strategies. *Transp. Res. Part C Emerg. Technol.*, 67:266–279.

Helbing, D. (2001). Traffic and related self-driven many-particle systems. *Rev. Mod. Phys.*, 73:1067–1141.

Herman, R. and Prigogine, I. (1971). *Kinetic theory of vehicular traffic*. Elsevier, New York.

Illner, R., Klar, A., and Materne, T. (2003). Vlasov-Fokker-Planck Models for Multilane Traffic Flow. *Commun. Math. Sci.*, 1(1):1–12.

Jacob, D. J. (2000). Heterogeneous chemistry and tropospheric ozone. *Atmos. Environ.*, 34(12):2131–2159.

Jacobson, M. Z. (2005). *Fundamentals of Atmospheric Modeling*. Cambridge University Press.

Kerner, B. S. and Konhäuser, P. (1993). Cluster effect in initially homogeneous traffic flow. *Phys. Rev. E*, 48:R2335–R2338.

Kerner, B. S. and Konhäuser, P. (1994). Structure and parameters of clusters in traffic flow. *Phys. Rev. E*, 50:54–83.

Klar, A. and Wegener, R. (2000). Kinetic Derivation of Macroscopic Anticipation Models for Vehicular Traffic. *SIAM J. Appl. Math.*, 60(5):1749–1766.

Knorr, F., Baselt, D., Schreckenberg, M., and Mauve, M. (2012). Reducing traffic jams via VANETs. *IEEE Transactions on Vehicular Technology*, 61(8):3490–3498.

Lebacque, J.-P., Mammar, S., and Haj-Salem, H. (2007). Generic second order traffic flow modelling. In Allsop, R. E., Bell, M. G. H., and Heydecker, B. G., editors, *Transportation and Traffic Theory*, Proc. of the 17th ISTTT, pages 755–776. Elsevier.

Lighthill, M. J. and Whitham, G. B. (1955). On kinematic waves II. A theory of traffic flow on long crowded roads. *Proc. Roy. Soc. A*, 229(1178):317–345.

Luspay, T., Kulcsar, B., Varga, I., Zegeye, S. K., De Schutter, B., and Verhaegen, M. (2010). On acceleration of traffic flow. In *Proceedings of the 13th International IEEE Conference on Intelligent Transportation Systems (ITSC 2010)*, pages 741–746. IEEE.

Manahan, S. (2017). *Environmental chemistry*. CRC press.

Nagel, K. and Schreckenberg, M. (1992). A cellular automaton model for freeway traffic. *J. Phys. I France*, 2:2221–2229.

Newell, G. F. (1961). Nonlinear Effects in the Dynamics of Car Following. *Oper. Res.*, 9(2):209–229.

Omidvarborna, H., Kumar, A., and Kim, D.-S. (2015). NO_x emissions from low-temperature combustion of biodiesel made of various feedstocks and blends. *Fuel Process. Technol.*, 140(Supplement C):113 – 118.

Panis, L. I., Broekx, S., and Liu, R. (2006). Modelling instantaneous traffic emission and the influence of traffic speed limits. *Sci. Total Environ.*, 371(1-3):270–285.

Phillips, W. F. (1979). A kinetic model for traffic flow with continuum implications. *Transportation Planning and Technology*, 5(3):131–138.

Piccoli, B., Han, K., Friesz, T. L., Yao, T., and Tang, J. (2015). Second-order models and traffic data from mobile sensors. *Transp. Res. Part C Emerg. Technol.*, 52(Supplement C):32 – 56.

Piccoli, B. and Tosin, A. (2011). *Vehicular Traffic: A Review of Continuum Mathematical Models*, pages 1748–1770. Springer New York, New York, NY.

Pipes, L. A. (1953). An Operational Analysis of Traffic Dynamics. *J. Appl. Phys.*, 24:274–281.

Richards, P. I. (1956). Shock Waves on the Highway. *Oper. Res.*, 4(1):42–51.

Sakai, S., Nishinari, K., and Iida, S. (2006). A new stochastic cellular automaton model on traffic flow and its jamming phase transition. *J. Phys. A: Math. Gen.*, 39:15327–15339.

Samaranayake, S., Glaser, S., Holstius, D., Monteil, J., Tracton, K., Seto, E., and Bayen, A. (2014). Real-Time Estimation of Pollution Emissions and Dispersion from Highway Traffic. *Comput.-Aided Civ. Inf.*, 29(7):546–558.

Song, F., Shin, J. Y., Jusino-Atresino, R., and Gao, Y. (2011). Relationships among the springtime ground–level NO_x, O_3 and NO_3 in the vicinity of highways in the US East Coast. *Atmos. Pollut. Res.*, 2(3):374–383.

Stern, R., Cui, S., Delle Monache, M. L., Bhadani, R., Bunting, M., Churchill, M., Hamilton, N., Haulcy, R., Pohlmann, H., Wu, F., Piccoli, B., Seibold, B., Sprinkle, J., and Work, D. B. (2018). Dissipation of stop-and-go waves via control of autonomous vehicles: Field experiments. *Transp. Res. Part C Emerg. Technol.*, 89:205–221.

Stern, R. E., Chen, Y., Churchill, M., Wu, F., Delle Monache, M. L., Piccoli, B., Seibold, B., Sprinkle, J., and Work, D. B. (2019). Quantifying air quality benefits resulting from few autonomous vehicles stabilizing traffic. *Transp. Res. Part D*, 67:361–365.

Sugiyama, Y., Fukui, M., Kikuchi, M., Hasebe, K., Nakayama, A., Nishinari, K., Tadaki, S., and Yukawa, S. (2008). Traffic jams without bottlenecks – Experimental evidence for the physical mechanism of the formation of a jam. *New J. Phys.*, 10:033001.

Talebpour, A. and Mahmassani, H. S. (2016). Influence of connected and autonomous vehicles on traffic flow stability and throughput. *Transp. Res. Part C Emerg. Technol.*, 71:143–163.

TRB Executive Committee (2011). Special Report 307: Policy Options for Reducing Energy and Greenhouse Gas Emissions from U.S. Transportation. Technical report, Transportation Research Board of the National Academies.

TRB Executive Committee (2013). Critical issues in transportation 2013. Technical report, Transportation Research Board of the National Academies.

Wang, M., Daamen, W., Hoogendoorn, S. P., and van Arem, B. (2016). Cooperative car-following control: Distributed algorithm and impact on moving jam features. *IEEE Transactions on Intelligent Transportation Systems*, 17(5):1459–1471.

Wang, T., Xue, L., Brimblecombe, P., Lam, Y., Li, L., and Zhang, L. (2017). Ozone pollution in China: A review of concentrations, meteorological influences, chemical precursors, and effects. *Sci. Total Environ.*, 575:1582–1596.

Work, D., Blandin, S., Tossavainen, O.-P., Piccoli, B., and Bayen, A. (2010). A traffic model for velocity data assimilation. *Appl. Math. Res. Express.*, 2010(1):1–35.

Zegeye, S., De Schutter, B., Hellendoorn, J., Breunesse, E., and Hegyi, A. (2013). Integrated macroscopic traffic flow, emission, and fuel consumption model for control purposes. *Transp. Res. Part C Emerg. Technol.*, 31:158–171.

Zhang, H. M. (2002). A non-equilibrium traffic model devoid of gas-like behavior. *Transp. Res. B*, 36:275–290.

Zhang, K. and Batterman, S. (2013). Air pollution and health risks due to vehicle traffic. *Sci. Total Environ.*, 450-451(Supplement C):307 – 316.